HHS Public Access

Author manuscript

Fertil Steril. Author manuscript; available in PMC 2016 July 01.

Published in final edited form as:

Fertil Steril. 2015 July ; 104(1): 225–234.e3. doi:10.1016/j.fertnstert.2015.04.021.

Stro-1/CD44 as putative human myometrial and fibroid stem cell markers

Aymara Mas, PhD[a,**], **Sangeeta Nair, DVM MS**[a,**], **Archana Laknaur, MS**[a], **Carlos Simón, MD, PhD**[b,c], **Michael P. Diamond, MD**[a], and **Ayman Al-Hendy, MD, PhD**[a,*]

[a]Department of Obstetrics and Gynecology, Georgia Regents University, Augusta, Georgia, USA

[b]Fundación Instituto Valenciano de Infertilidad, Instituto Universitario IVI-University of Valencia, INCLIVA, Valencia, Spain

[c]Department of Obstetrics and Gynecology, School of Medicine, Stanford University, California, USA

Abstract

Objective—To identify and characterize myometrial/fibroid stem cells by specific stem cell markers in human myometrium, and to better understand the stem cell contribution in the development of uterine fibroids.

Design—Prospective experimental human and animal study.

Setting—University research laboratory.

Patients—Women undergoing hysterectomy for treatment of symptomatic uterine fibroids.

Animals—Female NOD/*SCID*/IL-2Rγ^{null} mice.

Interventions—Identification and isolation of stem cells from human fibroids (F) and adjacent myometrium (MyoF) tissues using Stro-1/CD44 specific surface markers.

Main Outcome Measures—Flow cytometry, semi- quantitative polymerase chain reaction, clonogenicity assays, cell culture, molecular analysis, immunocyto- histochemistry, *in vitro* differentiation, and xenotransplantation assays.

Results—Using Stro-1/CD44 surface markers, we were able to isolate stem cells from MyoF and F tissues. The undifferentiated status of isolated cells was confirmed by the expression of ABCG2 transporter, as well as additional stem cell markers *OCT4, NANOG* and *GDB3*, and the low

*Corresponding author: Ayman Al-Hendy, Department of Obstetrics and Gynecology, Georgia Regents University, 1120 15th Street, Augusta 30912, Georgia, USA. aalhendy@GRU.edu.

**Both authors should be considered “similar in author order.”

SUPPLEMENTAL INFORMATION

Table S1. List of antibodies used for immunophenotypic analysis.

Table S2. List of primers used for cell line characterization.

Supplemental Figure S1. Viability graphs of SPIO-labeled MyoF and F cells

expression of steroid receptors ERα and PR-A/PR-B. Mesodermal cell origin was established by the presence of typical mesenchymal markers (CD90, CD105, and CD73) and absence of hematopoietic stem cell markers (CD34, CD45), and confirmed by the ability of these cells to differentiate *in vitro* into adipocytes, osteocytes and chondrocytes. Finally, their functional capability to form fibroid-like lesions was established in xenotransplantation mouse model. The injected cells labeled with superparamagnetic iron oxide (SPIO) were tracked by both magnetic resonance imaging (MRI) and fluorescence imaging, thus demonstrating the regenerative potential of putative fibroid stem cells *in vivo*.

Conclusion—We have demonstrated that Stro-1/CD44 can be used as specific surface markers to enrich a subpopulation of myometrial/fibroids cells, exhibiting key features of stem/progenitor cells. These findings offer a useful tool to better understanding the initiation of uterine fibroids, and may lead the establishment of effective therapeutic options.

Keywords

human myometrium; uterine fibroids/ leiomyomas; CD44/Stro-1; stem cells

INTRODUCTION

Uterine fibroids (UF) or leiomyomas are benign smooth muscle tumors of the uterus affecting 30–70% of reproductive age women (1). These tumors interfere with normal uterine functions and cause symptoms including prolonged and heavy menstrual bleeding, as well as infertility, recurrent abortion, and preterm labor (2–4). However, despite their high incidence and huge negative economic impact on the US health-care delivery system, the pathogenesis of this benign tumor remains unclear (5, 6).

Several genetic studies based on the unique isoenzyme pattern (7, 8), X-inactivation (9, 10) and DNA methylation-sensitive HUMARA assay (11) have demonstrated that uterine fibroids are monoclonal in origin. Accordingly, some studies have proposed that these benign tumors could originate from a single dysregulated myometrial smooth muscle stem cell, under the influence of ovarian hormones (6, 12, 13).

Although the cellular origin of uterine fibroids remains unknown, there is increasing evidence that putative stem/progenitor cells may be involved (6). Somatic stem cells (SSCs) are undifferentiated cells that reside in normal adult tissues as a restricted subpopulation in dormant o quiescent state. They are characterized by a high proliferative capacity, multipotentiality, capability of self-renewal and the ability to form the tissue that they originate from (14), contributing in this way to structural and functional tissue homeostasis (15).

The identification and characterization of SSCs is a great scientific challenge. In the last 7 years, several studies using the 5-bromo-2’-deoxyuridine (BrdU) and side population (SP) methods in murine and human myometrium have suggested the presence and functional relevance of SSCs in this tissue (16, 17). Analogously, it has also been demonstrated by the SP approach, that human uterine fibroids contain stem cells (also called tumor-initiating cells), retaining the ability to reconstitute tumors through asymmetric division (12, 18, 19).

Using microarray analysis on SP cells, we found that the top gene implicated targets in SP compared to the main population, were related to cancer, inflammatory response, and hematological system development and function (12). However, the SP based studies have limitation due to the heterogeneity of isolated cells. Furthermore, the scarcity and lack of distinctive morphological and cellular characteristics, such as defining cell surface markers, makes their identification and location a very complex task in most tissues, including uterine myometrium and fibroids.

The study presented here addresses the expression of Stro-1 and CD44 in human myometrium and fibroids. Stro-1 is a cell surface antigen that has shown robust enrichment for SSCs and nucleated erythroid precursors, but not by committed hematopoietic progenitors (20, 21). To date, several studies have reported that Stro-1 positive cell population exhibit enhanced cloning ability and elevated *in vitro* multipotency as compared to unsorted human bone marrow stromal cells (HBMSCs) (22). However, Stro-1-enriched SSCs remain highly heterogeneous (23, 24) and require additional refined selection using other markers to target specific myometrial/fibroid SSCs. CD44 is a multistructural multifunctional cell-surface glycoprotein involved in cell proliferation, differentiation and migration (25). This protein participates in a wide variety of cellular functions including lymphocyte activation, recirculation and hematopoiesis. These biological properties are essential for the physiological activities of normal cells, and are also associated with the pathologic activities of cancer cells. CD44+/CD24- expression is commonly used as a marker for breast cancer stem cells (CSCs) with stem-like characteristics (26). Splice variants of CD44 have also been detected in endometrial cells from women with endometriosis (27) and used as a prognostic indicator for survival time in epithelial ovarian cancer patients (28).

Although several studies have demonstrated the expression of Stro-1/CD44 in human myometrium (17, 25, 29), our aim was to establish Stro-1/CD44 as specific surface markers for human myometrial stem cells, which will assist to better understand the role of stem cells in the development of uterine fibroids. In this context, we have demonstrated along this study, through in vitro and in vivo approaches, the ability of these human Stro-1/CD44 positive myometrial and fibroid cells to differentiate into mesenchymal lineage cell types, and finally to form myometrial/fibroid like-tissues in an animal model.

MATERIALS AND METHODS

Human tissue collection and sample preparation

Samples of human myometrium and fibroids were collected from women undergoing hysterectomy or myomectomy for symptomatic uterine fibroids, (age range: 30–60) excluding other gynecological disorders or malignances. These women had not used any hormonal treatment for at least three months prior to the day of their surgery (day of sample collection). We consistently captured the menstrual phase for all the uterine tissue collection, based on subject history and subsequently, validated by endometrial histology. The samples used in this work were collected in the proliferative phase of the menstrual cycle. Use of human tissue specimens was approved by the Institutional Review Board and Ethics Committee of Meharry Medical College and all patients signed a written informed

consent. Consistently, we collected the fibroid tissues from relatively large fibroid lesions (≥ 6cm in diameter). We used lesions that did not show any central hemorrhage or necrosis. We also collected from the peripheral areas of the tumor (at least 1 cm from the pseudocapsule), as these areas traditionally exhibit robust growth. For the adjacent myometrium, we collected from areas with no visible abnormalities, at least 1 cm away from the closest fibroid lesions, to minimize possible hormonal or mechanical impact from adjacent fibroid lesions. In brief, myometrium and fibroid tissues were rinsed in wash buffer solution containing Hank's Balanced Salt Solution, HBSS (Life Technologies, Grand Island, NY) and 1% antibiotic- antimycotic solution (Life Technologies, Grand Island, NY). Samples were carefully manually minced into small pieces (<1 mm^3) and further dissociated using the gentleMACS dissociator (Milteny Biotec, CA). Then, they were suspended in enzyme buffer containing collagenase IV and DNAse I and digested overnight at 37°C by enzymatic means.

Isolation of stem cells from human myometrium and uterine fibroids

Magnetic bead selection was performed according to the manufacturer's instructions (Life Technologies, Grand Island, NY). Freshly isolated myometrial and fibroid cell suspensions were incubated with biotinylated and conjugated antibodies to CD-44 (BD Biosciences, San Jose, CA) and Stro-1 (R&D systems, Minneapolis, MN), diluted in isolation buffer containing Phosphate Buffered Saline (PBS, Sigma- Aldrich, St. Louis, MO), and supplemented with 0.1% Bovine Serum Albumin (BSA, Sigma- Aldrich, St. Louis, MO) and 2 mM of Ethylene diamine tetraacetic acid, EDTA. Dynabeads FlowComp (Life Technologies, Grand Island, NY) were then added and tubes containing myometrial and fibroid cells were placed in a magnet to separate the candidate Stro-1/CD44 positive (Stro-1^+/$CD44^+$) cells from the supernatant containing non target cells, repeating this step in triplicate to remove any residual beads. Finally, Stro-1^+/$CD44^+$ myometrial (Stro-1^+/$CD44^+$MyoF), fibroid (Stro-1^+/$CD44^+$F) cells, (considered as putative myometrial/fibroid stem cells) and primary myometrial/ fibroid (PrMyoF/ PrF) cells, (categorized by the absence of Stro-1 and CD44), were cultured separately in Dulbecco's modified Eagle's medium (DMEM-F12, Sigma-Aldrich, St. Louis, MO) with 10% fetal bovine serum (FBS, Stem Cell Technologies, Canada) and 1% antibiotic-antimycotic (Life Technologies, NY), and plated in collagen coated dishes.

Characterization of myometrial/fibroid stem cells by flow cytometric analysis

Stro-1^+/$CD44^+$MyoF and Stro-1^+/$CD44^+$F cultured cells were dissociated from the collagen coated dishes by using non-enzymatic cell dissociation buffer (Gibco). They were washed and resuspended in cold stain buffer in order to perform the immunophenotypic analysis using CD90 (10 μl), CD73 (5 μl), and CD105 (10 μl) for mesenchymal stem cells; CD34 (10 μl) and CD45 (15 μl) for hematopoietic stem cells; CD31 (10 μl) for endothelial cells (antibodies are detailed in Supplemental Table S1). Similarly, isotype controls were prepared for each antibody in separate aliquots. The black colored line depicts the unstained cells and the overlapping line is the isotype control. The line marked with the arrow is the peak for the antibody specific positive cells. The immunophenotypic analysis was performed in a BD FACSCalibur flow cytometer system (Beckman-Coulter, CA, USA).

Isolation of RNA and reverse transcription PCR

Total RNA was extracted from Stro-1^{+}/CD44^{+}MyoF, Stro-1^{+}/CD44^{+}F and primary cells (PrMyoF/ PrF) from 100 mm confluent dishes. Qiagen kit (Qiagen, CA) was used according to the manufacturer's recommended protocol and semi-quantitative PCR was carried out using an Eppendorf MasterPro thermal cycler under the following conditions: 56°C and 28 cycles for Octamer-binding transcription factor 4 (*OCT-4*), *Nanog*, DNA cytosine-5-methyltransferase 3 beta (*DNMT3B*), Growth differentiation factor-3 (*GDF3*), *GABR3*, and *GAPDH* as an internal control in all the gene expression studies. Bone marrow stem cells were also used as a positive control for undifferentiated markers. ATP-binding cassette transporter G2 (*ABCG2*) and hormone receptors such as estrogen receptor-alpha (*ESR1*), and progesterone receptor (*PR*) were carried out separately, at 59°C and 30 cycles PCR conditions. All products were run on a 1.5% agarose electrophoresis gel. Primers used for PCR amplification are listed in Supplemental Table S2.

In vitro colony assay

Stro-1^{+}/CD44^{+}MyoF, Stro-1^{+}/CD44^{+}F and primary cells (PrMyoF/ PrF) were seeded in duplicate in 6-well gelatin coated plates at 156 cells/cm2 clonal density. Cells were grown in DMEM-F12 media (Sigma-Aldrich, St. Louis, MO) containing 12% FBS (Stem cell Technologies, Canada) and 1% antibiotic-antimycotic (Life Technologies, NY) in a hypoxia environment (2% O_2, 37°C, 5% CO_2, 90% humidity) (30). After two weeks, media was removed from the wells and cells were rinsed with phosphate-buffered saline $Ca^{+2}Mg^{+2}$ free (Life Technologies, NY), and fixed with 70% ethanol. Clones were stained with 1% methylene blue for 15–30 minutes and counted under a stereomicroscope. Cloning efficiency (CE) was calculated using the standard formula: CE= (number of clones/ number of cells seeded) x 100. The mean and SEM were obtained from each clonal density and SEM were calculated for each cell type. Statistical analysis of the data was performed with GraphPad Prism software's and t- test was used to evaluate the significance of the samples (95% confidence) with statistical significance set at a p-value< 0.05.

In vitro differentiation assays

Adipogenic, osteogenic and chondrogenic differentiation kits (Lonza, Walkersville, MD) were used for differentiating the isolated Stro-1^{+}/CD44^{+}MyoF and Stro-1^{+}/CD44^{+}F cells into adipose cells, osteocytes and chondrocytes respectively.

To induce adipogenic and osteogenic differentiation, cells were seeded at $2x10^5$ cells/ well in 6 well-plates under induction media conditions, according to the manufacturer's protocols. For *in vitro* chondrogenic differentiation, $5x10^5$ cells were cultured as a pellet micromass under induction media conditions, according to the manufacturer's protocols. A mesenchymal stem cell line (MSC) (ATCC, VA, USA) was used as positive control for the differentiation process, and Stro-1^{+}/CD44^{+}MyoF and Stro-1^{+}/CD44^{+}F $^{+}$ cells were also treated with maintenance media (without inducing factors) as the negative control for this technique. In all cases, during the differentiation protocol, cells were maintained under normoxic conditions (18%–20% O2, 37°C, 5% CO2 , 90% humidity), changing media every 3 or 4 days for 4 weeks. To confirm the differentiation process, cells were fixed in 4% paraformaldehyde (PFA) and stained with Oil red-O (adipocytes), Alizarin (osteocytes) and

Toluidine Blue (chondrocytes) respectively. Stained cells were examined under a Zeiss AxioVert microscope (Zeiss, NY, USA), and images were captured using an Axiocam digital camera (Zeiss, NY, USA).

Molday Ion Rhodamine staining, flow cytometry analysis and preparation of cell graft

Stro-1^+/$CD44^+$MyoF and Stro-1^+/$CD44^+$F cells were labeled using fluorescent iron-oxide nanoparticles to track them within the animal model. Our methodology included the use of the "Molday Ion Rhodamine B" (MIRB, Biopal) technique, a new superparamagnetic iron oxide (SPIO) contrast agent specifically formulated for cell labelling and is readily internalized by non-phagocytic cells (31). Moreover, it is labeled with Rhodamine B (RhoB) fluorescent dye, which allows labeled cells to be sorted by flow cytometry (555–620 nm) and detected by Prussian Blue staining in paraffin embedded tissue due to the presence of iron deposits. Effects of MIRB on cell viability were assessed, and finally 30 μg/ml was added to cell suspensions and incubated for 16 hours at 37°C (Supplemental figure S1). Cells were then viewed by a fluorescent Nikon microscope and suspended on PBS for flow cytometry analysis.

After flow cytometry analysis, positive Stro-1^+/$CD44^+$MyoF and Stro-1^+/$CD44^+$F RhoB cells as well as cells from immortalized human uterine fibroid cell line (HuLM cells) provided by Dr. Darlene Dixon (32), were collected and suspended into rat-tail collagen (type I) solution (BD Bioscience, San Jose, CA) at 10^6 cells per 10 μl (33). Cell pellets were incubated at 37°C overnight as a floating-culture, and mixed with an equal volume of high concentrated matrigel HC (BD Bioscience) supplemented with epidermal growth factor (EGF, 0.5 ng/ml, Invitrogen, Carlsbad, CA), basic fibroblast growth factor (bFGF, 2 ng/ml, Invitrogen, Carlsbad, CA) and insulin (5 μg/ μl, Sigma-Aldrich, St. Louis, MO).

Generation of xenografts

All experiments using female non-obese diabetic mice (NOD-SCID) (strain code394; NOD.CB17- $Prkdc^{scid}$/NcrCrl, Charles River Laboratories) were conducted in accordance with the Institutional Review Board and the Ethics Committee of Georgia Regents University (GRU). This protocol was approved by the Committee on the Ethics of Animal experiments of Georgia Regents University (GRU). Xenotransplantation assays were performed based on the injection of Stro-1^+/$CD44^+$MyoF and Stro-1^+/$CD44^+$F cells under the kidney capsule. HuLM cells were used as negative control. After kidney externalization, 16 mice (aged 5–6 weeks) were injected beneath the renal capsule with single-cell suspensions ($5x10^5 - 1x10^6$ cells) from Stro-1^+/$CD44^+$MyoF and Stro-1^+/$CD44^+$F cell grafts, either injected alone or mixed with myometrial/ fibroid primary cells (PrMyoF/ PrF) in those animals treated with 17-β Estradiol (0.1 mg E2, Innovative Research of America, Sarasota, FL) and progesterone (50 mg P4, Innovative Research of America, Sarasota, FL). All xenotransplanted mice were monitored twice a week and maintained in specific pathogen-free (SPF) facilities until sacrificed 8 weeks (60 days) after the injection.

MRI characterization and image evaluation

In the final phase of our *in vivo* experiment, we followed the protocol of Belmar-Lopez et al, in which mice were anesthetized with oxygen (1 l/min) containing 4% isofluorane, and

maintained with 1 to 1.5% isofluorane in O_2 (34). Simultaneously, longitudinally imaging with high field anatomic MRI were performed. T2-weighted spin-echo anatomical images were acquired by rapid acquisition with relaxation enhancement (RARE) sequence in axial (12 slices) and sagittal (8 slices) orientations, corresponding to an in-plane resolution of 117 x 117 μm^2 and slice thickness of 1.00 mm.

After MRI confirmation, animals were sacrificed and kidneys were removed for fluorescent imaging by using the IVIS (Xenogen, Lincolnshire, United Kingdom) for 120 seconds. To quantify fluorescence, identical regions of interest were positioned to encircle each luminescent lesion, and the integrated flux of photons (photons per second) within each region of interest was determined using the Living Images software package (Xenogen, Lincolnshire, United Kingdom). Data were normalized to fluorescence recorded at the initiation of treatment for each animal.

Immunostaining and histological analysis of xenograft tissue

Histological analyses were performed routinely for all human myometrial/fibroid-like tissues generated in the kidneys of the mice. Samples were fixed in 10% buffered formaldehyde for 24h, dehydrated in an ethanol series, cleared in xylene and embedded in paraffin. Sections of 4 μm were obtained from the blocks for staining with haematoxylin and eosin (H&E, Sigma-Aldrich). Prussian blue staining (Sigma-Aldrich) was used to detect labeled iron particles in the cells, in accordance with the manufacturer's instructions. Immunohistochemistry analyses of these samples were conducted for several antibodies i.e. Ki67 (Santa Cruz, Dallas), human progesterone receptor (Thermo Scientific, Fremont, CA), actin alpha 2 smooth muscle antibody (NovusBio, Littleton, CO) and collagen I (NovusBio, Littleton, CO). Finally, immunolocalization of specific cell populations were analyzed, visualized and photographed using the EVOS® XL Core Cell Imaging System (Life Technologies, NY).

Data analysis

Flow cytometric data were analyzed using FlowJo 8.7.3 software. Pearson's correlation was performed using GraphPad Prism version 5.00 for Windows (GraphPad Software, San Diego, USA). Unpaired Student's t test with 95% confidence intervals was utilized for comparative analysis, with a significance level of $p\text{-value} < 0.05$ considered statistically significant.

RESULTS

Isolation and characterization of the human myometrial/fibroid Stro-1^+/$CD44^+$ stem cells

Stro-1^+/$CD44^+$ single-cell suspensions were isolated from MyoF or F tissues using magnetic Dynabeads FlowComp (Life Technologies, Grand Island, NY) and primary cells (PrMyoF/ PrF) from corresponding tissue were used as control. The expression of typical undifferentiated stem cell-related genes was validated by semi-quantitative PCR, obtaining a molecular profile in isolated human Stro-1^+/$CD44^+$MyoF and Stro-1^+/$CD44^+$F consistent with undifferentiated cell status like *OCT-4*, *Nanog*, *DNMT3B* and *GDF3 versus* human primary cells (PrMyoF/ PrF). (Fig. 1A). Moreover, isolated human Stro-1^+/$CD44^+$MyoF and

Stro-1$^+$/CD44$^+$F also expressed ABCG2 transporter similar to the SP phenotype as we have previously reported (12). At the mRNA level, important hormonal receptors such as *ER*α and *PR* also showed a specific pattern with the highest expression in primary cells (PrMyoF/ PrF). These results indicate that Stro-1$^+$/CD44$^+$MyoF and Stro-1$^+$/CD44$^+$F are not yet hormonally committed (Fig. 1B).

Immunophenotype analysis of Stro-1$^+$/CD44$^+$MyoF cells revealed that mesenchymal lineage markers were present in 94.32% for CD90, 77.52% for CD105, and 93.78% for CD73 (Fig. 1C). In Stro-1$^+$/CD44$^+$F cells (Stro-1$^+$/CD44$^+$) the expression of these markers was present in 77.72% for CD90, 54.81% for CD105 and 94% for CD73. As expected, the expression of typical hematopoietic markers CD34, CD45 or endothelial markers like CD31 was barely detectable (Fig. 1C) in both cell populations. These results strongly suggest that Stro-1$^+$/CD44$^+$MyoF and Stro-1$^+$/CD44$^+$F cells possess a mesenchymal phenotype.

Clonogenic assay

Accumulated evidences indicate a clonal origin of uterine fibroids probably from a deranged myometrial stem cell (7– 11). Stro-1$^+$/CD44$^+$MyoF and Stro-1$^+$/CD44$^+$F cells and primary cells (PrMyoF/ PrF) were seeded in triplicate at 156 cells/ cm^2 under hypoxic conditions (2% O_2, 37°C, 5% CO_2, 90% humidity) to determine clonogenic efficiency (CE). After 15 days, results confirmed that Stro-1$^+$/CD44$^+$F cells showed significantly higher CE (0.15%) *versus* primary cells (PrF) (0.08%) ($P<0.05$). Similarly, the clonogenicity of Stro-1$^+$/ CD44$^+$MyoF (0.22%) was higher as compared with primary cells (PrMyoF) (0.12%), however, the differences were not statistically significant ($P=0.1$, Fig. 2A).

In vitro multipotential differentiation

One of the more remarkable features of SSC cells is their plasticity and ability to differentiate to specific lineages related to the germ layer that they are derived from. For this purpose, we examined the *in vitro* potential of the Stro-1$^+$/CD44$^+$MyoF and Stro-1$^+$/ CD44$^+$F cell populations undergoing adipogenic, osteogenic and chondrogenic differentiation. A bone marrow mesenchymal stem cell line (MSC) (ATCC, VA, USA) was used as a positive control. In the presence of adipogenic induction media MSC, Stro-1$^+$/ CD44$^+$MyoF and Stro-1$^+$/CD44$^+$F cells exhibited an accumulation of lipid droplets, confirmed by the cytoplasmic staining with Oil Red-O. In contrast, cells treated with maintenance media did not stain in the presence of this dye, as evidenced by the absence of lipid droplets (Fig. 2B, upper). Similarly, Stro-1$^+$/CD44$^+$MyoF and Stro-1$^+$/CD44$^+$F cells treated with osteogenic induction media were positive for Alizarin Red dye, specific for mineralized tissues, while cells treated with control media were negative (Fig. 2B, middle). Finally, Toluidine Blue staining of MSC, Stro-1$^+$/CD44$^+$MyoF and Stro-1$^+$/CD44$^+$F cells treated with chondrogenic induction media showed the characteristic metachromasia specific of extracellular matrix components, while undifferentiated or fibrous tissue was stained in blue (Fig. 2B, lower). Therefore, similar to our prior results obtained with SP cells (12), Stro-1$^+$/CD44$^+$MyoF and Stro-1$^+$/CD44$^+$F cells were able to differentiate into adipocytes, osteocytes and chondrocytes.

Reconstruction of human fibroid-like tissue from SPIO-labeled Stro-1$^+$/CD44$^+$ MyoF and F cells in vivo

To validate the ability of Stro-1$^+$/CD44$^+$MyoF and Stro-1$^+$/CD44$^+$F cells to form corresponding (myometrial or fibroid) tissues, respectively, which is the hall mark of stem cells, we used a kidney capsule mouse model as we have described previously (12). To be able to track these cells in vivo, they were labelled ex vivo with SPIO as we have described previously (12) and as depicted in the materials and methods section. The viability of SPIO-labeled Stro-1$^+$/CD44$^+$MyoF and Stro-1$^+$/CD44$^+$F cells was determined by the Trypan blue/ 7-Amino Actinomycin D (7-ADD) exclusion assay. At varying concentrations, the percentage of living cells with rhodamine B positive signal at 575 nm was consistently around 85–90% in Stro-1$^+$/CD44$^+$MyoF or Stro-1$^+$/CD44$^+$F cells respectively (Supplemental figure S1), demonstrating that labelling with SPIO did not affect cell viability and proliferation.

After injection of SPIO labelled Stro-1$^+$/CD44$^+$MyoF, Stro-1$^+$/CD44$^+$F and HuLM cells under the mouse kidney capsule, mice were maintained for eight-weeks with hormonal supplement (17-β estradiol and progesterone pellets). To confirm whether labeled injected cells were able to differentiate and form corresponding tissues under the kidney capsule, two imaging techniques were performed: MRI and fluorescence imaging using IVIS (Xenogen, Lincolnshire, United Kingdom). The MRI, was used to demonstrate the recruitment of SPIO-labeled MyoF and F cells into the kidney xenografts, and resulted in a decrease in signal intensity (SI) and visualization of darker areas in fibroid-like tissue sites (Fig. 3A, middle & right panel). No decrease in SI was detected in immortalized human leiomyoma HuML cells (Fig. 3A, left panel).

At the completion of the experiment, kidneys were removed, fixed, sectioned, and stained with Rhodamine using the IVIS (Xenogen, Lincolnshire, United Kingdom) for 120 seconds. The images obtained displayed a color spectrum, with the weakest signal being in blue and the strongest in red. In whole-kidney scans of control mice (injected with unlabeled HuML cells) an endogenous (basal) expression signal was observed. However, a higher accumulation of SPIO- labeled Stro-1$^+$/CD44$^+$MyoF and Stro-1$^+$/CD44$^+$F was detected at kidney sites in animals that were injected with the myometrial stem cells alone, resulting with the highest expression signal when they were in combination with primary cells (PrMyoF/ PrF) (Fig. 3B, Fig. 4B).

After image evaluation, mice kidneys were processed for immuno-staining and histological analysis of the reconstructed xenograft tissue. As shown in Fig. 3B and Fig. 4B, Stro-1$^+$/ CD44$^+$MyoF and Stro-1$^+$/CD44$^+$F cells either alone or in combination with primary cells (PrMyoF/ PrF) have the ability to form human fibroid like-tissue *in vivo*, and appear to be macroscopically (Fig. 3B, Fig. 4B) and histologically (Fig. 3C, Fig. 4C) similar to human fibroids. Stro-1$^+$/CD44$^+$MyoF cells injected alone were able to grow as cell grafts, however tumor volume was not as large as Stro-1$^+$/CD44$^+$MyoF in combination with primary cells (PrMyoF/ PrF) or Stro-1$^+$/CD44$^+$F in combination with primary cells (PrMyoF/ PrF). Intense blue clusters of Prussian blue staining was detected in xenograft tissues from human SPIO-labeled Stro-1$^+$/CD44$^+$MyoF and Stro-1$^+$/CD44$^+$F cells (Fig. 3C, Fig. 4C). Positive

Ki67 staining in xenograft tissues, demonstrated a moderate proliferative pattern in all Stro-1$^+$/CD44$^+$MyoF and Stro-1$^+$/CD44$^+$F inoculated kidneys. To further assess the human origin and expression of hormonal receptors in the reconstructed xenografts, human progesterone receptor (hPR), actin alpha-2 smooth muscle and collagen I staining, were performed and detected in the formed myometrium and fibroid-like lesions. Collectively, these data support the important role of steroid hormones in tumor formation as well as the presence of human myometrial/fibroid cells and extracellular matrix components (ECM), respectively (Fig. 3C and Fig. 4C).

CONCLUSIONS

To date, the primary approach to treatment of uterine fibroids is either surgical through the direct removal (hysterectomy or myomectomy) or induction of necrosis using nonsurgical radiological techniques (3, 35). Although GnRH analogues and progesterone receptor (PR) modulators are used as potential non-surgical treatments for this disease (36, 37), novel non-invasive therapeutic options must come from a basic understanding of the underlying pathophysiology of this disease (38). Furthermore, the high rate of fibroid recurrence after all of the above modalities (except hysterectomy) are attributed to persistence of tumor forming stem cells (4). Thus further characterization of fibroid stem cells will conceivably lead to better and more targeted and effective treatment option for this common disease.

By characterizing the putative myometrial/ fibroid stem cell populations with novel markers like Stro-1$^+$/CD44$^+$, we are setting the stage not only for innovative treatment options for this disease but also for its prevention. This study provides novel data showing that myometrial/ fibroid stem cell populations can be selected for purification using magnetic beads, as well as flow cytometry sorting (12, 13). A major advantage of bead selection is the rapid and simple isolation protocol which precludes the need for prolonged flow cytometry preparation steps and access to sophisticated machines and software, saving time and reducing costs (39).

Through the molecular characterization of Stro-1$^+$/CD44$^+$MyoF and Stro-1$^+$/CD44$^+$F cells, we have demonstrated the undifferentiated status of these cells, as well as, the low expression of sex steroid hormonal receptors (*ER*α and *PR*), thereby indicating non-committal hormonal nature. This is consistent with prior reports using the SP approach (12, 18). Moreover, the mesenchymal lineage commitment of Stro-1$^+$/CD44$^+$MyoF and Stro-1$^+$/CD44$^+$F cells has also been demonstrated, assessed by the expression of mesenchymal markers like CD90, CD105, and CD73, as well as by the absence of typical markers for the hematopoietic lineage (CD45 and CD34) and endothelial progenitor (CD31).

Yet another novel finding was the observation that Stro-1$^+$/CD44$^+$MyoF and Stro-1$^+$/CD44$^+$F cells proliferate efficiently *in vitro* under hypoxic conditions like SP cells (12, 17). Thus, it is feasible to speculate that under in vivo hypoxic conditions, fibroids could originate from a single dysregulated Stro-1$^+$/CD44$^+$ myometrial cell under the influence of ovarian sex hormones and with the added contribution of specific gene mutations such as Med12 (13, 40).

Somatic stem cells are defined as self-renewable and multipotent progenitor cells, which have the ability to differentiate into different cell types from a specific lineage (15). Throughout this study, we have found that Stro-1$^+$/CD44$^+$MyoF and Stro-1$^+$/CD44$^+$F cells were able to differentiate towards mesenchymal specific lineages like adipocytes, osteocytes and chondrocytes under proper inducting conditions, as demonstrated by the morphology and specific staining patterns.

The hallmark of stemness of these cells was based on their ability to reconstruct myometrial/ fibroid-like tissue in immunodeficient mice. Labeling cells with super-paramagnetic iron oxide (SPIO) nanoparticles allowed us the ability to track labeled cells within targeted tissues following cell injection using magnetic resonance imaging (MRI) and fluorescent imaging analysis (41). We confirmed the reconstruction of myometrial/ fibroid like tissue at the injection site under the kidney capsule by histological features, demonstrating the crucial interaction of Stro-1$^+$/CD44$^+$MyoF and Stro-1$^+$/CD44$^+$F with with primary cells (PrMyoF/ PrF) to create the proper niche for tissue regeneration and formation. Supporting this proliferative pattern, the Ki67 staining performed in xenograft tissues showed a moderate proliferative model uniquely observed in reconstructed areas. The presence of hPR in reconstructed tissues also confirms the hypothesis that estradiol could maintain progesterone receptor levels and that it is progesterone through its receptor that promotes myometrial/ fibroid growth (42). Finally, the expression of actin alpha-2 smooth muscle and collagen I, further confirmed the myometrial/fibroid-like composition with high extracellular matrix production. The fact that significantly larger lesions (Fig 3B and 4B) were observed only when a mixture of the primary and stem cells are inoculated together, support the paracrine pattern of signaling that was reported recently in fibroid lesions and have been established for several other hormonal dependent tumors (26, 39).

In summary, the results of this study pose a strong argument supporting the identification and characterization of Stro-1/CD44 as new specific human myometrial/ fibroid stem cell markers. Indeed, these Stro-1$^+$/CD44$^+$MyoF and Stro-1$^+$/CD44$^+$F cells possess preferential hypoxic proliferation ability, are mesenchymal in origin and lineage, as well as give rise to myometrial/fibroid like tissue in appropriate *in vivo* animal model. In conclusion, the use of Stro-1/CD44 as specific surface markers to target human fibroid stem cells with technologies such as gene therapy or nanoparticles, could improve the durability of fibroid management. Finally, these cells offer a useful tool to better understand of the origin and initiation of uterine fibroids, which can in turn foster the development of innovative and potentially more effective, therapeutic options by targeting myometrial/fibroid SSCs.

Supplementary Material

Refer to Web version on PubMed Central for supplementary material.

Acknowledgements

The authors are grateful to Dr. Ali Eroglu, Department of Neuroscience & Regenerative Medicine and all of the members from the Histology Core Lab and Imaging Core, Georgia Regents University, for their support in the preparation of this manuscript.

This work was supported in part by the National Institutes of Health grant HD046228-11.

REFERENCES

1. Zimmermann A, Bernuit D, Gerlinger C, Schaefers M, Geppert K. Prevalence, symptoms and management of uterine fibroids: an international internet-based survey of 21,746 women. BMC Womens Health. 2012; 12:6. [PubMed: 22448610]
2. Stewart EA. Uterine fibroids. Lancet. 2001; 357:293–298. [PubMed: 11214143]
3. Parker WH. Uterine myomas: management. Fertil Steril. 2007; 88(2):255–271. Review. [PubMed: 17658523]
4. Mas A, Cervello I, Gil-Sanchis C, Simón C. Current understanding of somatic stem cells in leiomyoma formation. Fertil Steril. 2014; 102(3):613–620. [PubMed: 24890270]
5. Cardozo ER, Clark AD, Banks NK, Henne MB, Stegmann BJ, Segars JH. The estimated annual cost of uterine leiomyomata in the United States. Am J Obstet Gynecol. 2012; 206:211. e1–9. [PubMed: 22244472]
6. Bulun SE. Uterine Fibroids. N Engl J Med. 2013; 369(14):1344–1355. [PubMed: 24088094]
7. Linder D, Gartler SM. Glucose-6-phosphate dehydrogenase mosaicism: utilization as a cell marker in the study of leiomyomas. Science. 1965; 150:67–69. [PubMed: 5833538]
8. Townsend DE, Sparkes RS, Baluda MC, McClelland G. Unicellular histogenesis of uterine leiomyomas as determined by electrophoresis by glucose-6-phosphate dehydrogenase. Am J Obstet Gynecol. 1970; 107(8):1168–1173. [PubMed: 5458572]
9. Canevari RA, Pontes A, Rosa FE, Rainho CA, Rogatto SR. Independent clonal origin of multiple uterine leiomyomas that was determined by X chromosome inactivation and microsatellite analysis. Am J Obstet Gynecol. 2005; 193:1395–1403. [PubMed: 16202732]
10. Cai YR, Diao XL, Wang SF, Zhang HAT, Su Q. X-chromosomal inactivation analysis of uterine leiomyomas reveals a common clonal origin of different tumor nodules in some multiple leiomyomas. Int J Oncol. 2007; 31:1379–1389. [PubMed: 17982665]
11. Holdsworth-Carson SJ, Zaitseva M, Vollenhoven BJ, Rogers PA. Clonality of smooth muscle and fibroblast cell populations isolated from human fibroid and myometrial tissues. Mol Hum Reprod. 2014; 20(3):250–259. [PubMed: 24243625]
12. Mas A, Cervelló I, Gil-Sanchis C, Faus A, Ferro J, Pellicer A, et al. Identification and characterization of the human leiomyoma side population as putative tumor-initiating cells. Fertil Steril. 2012; 98(3):e6751.
13. Drosch M, Schmidt N, Markowski DN, Zollner TM, Koch M, Bullerdiek J. The CD24hi smooth muscle subpopulation is the predominant fraction in uterine leiomyomas. Mol Hum Reprod. 2014; 20(7):664–676. [PubMed: 24657878]
14. Fuchs E, Tumbar T, Guasch G. Socializing with the neighbors: stem cells and their niche. Cell. 2004; 116:769–778. [PubMed: 15035980]
15. Daley GQ. Stem cells: roadmap to the clinic. J Clin Invest. 2010; 120(1):8–10. Review. [PubMed: 20051631]
16. SzoteK P, Chang HL, Zhang L, Preffer F, Dombkowski D, Donahoe PK, et al. Adult mouse myometrial label-retaining cells divide in response to gonadotropin stimulation. Stem Cells. 2007; 25(5):1317–1325. [PubMed: 17289934]
17. Ono M, Maruyama T, Masuda H, Kajitani T, Nagashima T, Arase T, et al. Side population in human uterine myometrium displays phenotypic and functional characteristics of myometrial stem cells. Proc Natl Acad Sci USA. 2007; 104:18700–18705. [PubMed: 18003928]
18. Ono M, Qiang W, Serna VA, Yin P, Coon JS5th, Navarro A, et al. Role of stem cells in human uterine leiomyoma growth. PLoS One. 2012; 7(5):e36935. [PubMed: 22570742]
19. Ono M, Yin P, Navarro A, Moravek MB, Coon VJ, Druschitz SA, et al. Inhibition of canonical WNT signaling attenuates human leiomyoma cell growth. Fertil Steril. 2014; 101(5):1441–1449. [PubMed: 24534281]
20. Simmons PJ, Torok-Storb B. Identification of stromal cell precursors in human bone marrow by a novel monoclonal antibody, STRO-1. Blood. 1991; 78(1):55–62. [PubMed: 2070060]
21. Zannettino AC, Paton S, Kortesidis A, Khor F, Itescu S, Gronthos S. Human multipotential mesenchymal/stromal stem cells are derived from a discrete subpopulation of STRO-1bright/

CD34/CD45-/Glycophorin-A-bone marrow cells. Haematologica. 2007; 92(12):1707–1708. [PubMed: 18055998]

22. Gothard D, Greenhough J, Ralph E, Oreffo R. Prospective isolation of human bone marrow stromal cell subsets: A comparative study between Stro-1-, CD146- and CD105-enriched populations. J Tissue Eng. 2014; 5:2041731414551763. [PubMed: 25383172]
23. Phinney DG, Prockop DJ. Concise review: mesenchymal stem/multipotent stromal cells: the state of transdifferentiation and modes of tissue repair - current views. Stem Cells. 2007; 25(11):2896–2902. [PubMed: 17901396]
24. Pevsner-Fischer M, Levin S, Zipori D. The origins of mesenchymal stromal cell heterogeneity. Stem Cell Rev. 2011; 7(3):560–568. [PubMed: 21437576]
25. Poncelet C, Walker F, Madelenat P, Bringuier AF, Scoazec JY, Feldmann G, et al. Expression of CD44 standard and isoforms V3 and V6 in uterine smooth muscle tumors: a possible diagnostic tool for the diagnosis of leiomyosarcoma. Hum Pathol. 2001; 32(11):1190–1196. [PubMed: 11727257]
26. Li F, Tiede B, Massagué J, Kang Y. “Beyond tumorigenesis: cancer stem cells in metastasis ”. Cell Res. 2007; 17(1):3–14. [PubMed: 17179981]
27. Griffith JS, Liu YG, Tekmal RR, Binkley PA, Holden AE, Schenken RS. Menstrual endometrial cells from women with endometriosis demonstrate increased adherence to peritoneal cells and increased expression of CD44 splice variants. Fertil Steril. 2010; 93(6):1745–1749. [PubMed: 19200980]
28. Sillanpää S, Anttila MA, Voutilainen K, Tammi RH, Tammi MI, Saarikoski SV, et al. CD44 expression indicates favorable prognosis in epithelial ovarian cancer. Clin Cancer Res. 2003; 9(14):5318–5324. [PubMed: 14614016]
29. Gálvez BG, Martín NS, Salama-Cohen P, Lazcano JJ, Coronado MJ, Lamelas ML, et al. An adult myometrial pluripotential precursor that promotes healing of damaged muscular tissues. In Vivo. 2010; 24(4):431–441. [PubMed: 20668309]
30. Chang HL, Senaratne TN, Zhang L, Szotek PP, Stewart E, Dombkowski D, et al. Uterine leiomyomas exhibit fewer stem/progenitor cell characteristics when compared with corresponding normal myometrium. Reproductive Sci. 2010; 17:158–167.
31. Addicott B, Willman M, Rodriguez J, Padgett K, Han D, Berman D, et al. Mesenchymal stem cell labeling and in vitro MR characterization at 1.5 T of new SPIO contrast agent: Molday ION Rhodamine-B™. Contrast Media Mol Imaging. 2011; 6(1):7–18. [PubMed: 20690161]
32. Carney SA, Tahara H, Swartz CD, Risinger JI, He H, Moore AB, et al. Immortalization of human uterine leiomyoma and myometrial cell lines after induction of telomerase activity: molecular and phenotypic characteristics. Lab Invest. 2002 Jun; 82(6):719–728. [PubMed: 12065682]
33. Ishikawa H, Ishi K, Ann Serna V, Kakazu R, Bulun SE, Kurita T. Progesterone Is Essential for Maintenance and Growth of Uterine Leiomyoma. Endocrinology. 2010; 151(6):2433–2442. [PubMed: 20375184]
34. Belmar-Lopez C, Mendoza G, Oberg D, Burnet J, Simon C, Cervelló I, et al. Tissue-derived mesenchymal stromal cells used as vehicles for anti-tumor therapy exert different in vivo effects on migration capacity and tumor growth. BMC Med. 2013; 11:139. [PubMed: 23710709]
35. Bouwsma EV, Hesley GK, Woodrum DA, Weaver AL, Leppert PC, Peterson LG, et al. Comparing focused ultrasound and uterine artery embolization for uterine fibroids-rationale and design of the Fibroid Interventions:reducing symptoms today and tomorrow (FIRSTT) trial. Fertil. Steril. 2011; 96(3):704–710. [PubMed: 21794858]
36. Bouchard P, Chabbert-Buffet N, Fauser BC. Selective progesterone receptor modulators in reproductive medicine: pharmacology, clinical efficacy and safety. Fertil. Steril. 2011; 96(5): 1175–1189. [PubMed: 21944187]
37. Islam MS, Protic O, Stortoni P, Grechi G, Lamanna P, Petraglia F, et al. Complex networks of multiple factors in the pathogenesis of uterine leiomyoma. Fertil Steril. 2013; 100(1):178–193. [PubMed: 23557758]
38. Stewart EA. New science will move fibroid therapies into the 21st century. Fertil. Steril. 2012; 98(3):604–605. [PubMed: 22704631]

39. Masuda H, Anwar SS, Bühring HJ, Rao JR, Gargett CE. A novel marker of human endometrial mesenchymal stem-like cells. Cell Transplant. 2012; 21(10):2201–2214. [PubMed: 22469435]

40. Zhou S, Yi T, Shen K, Zhang B, Huang F, Zhao X. Hypoxia: the driving force of uterine myometrial stem cells differentiation into leiomyoma cells. Med. Hypotheses. 2011; 77:985–986. [PubMed: 21903341]

41. Liu J, Stace-Naughton A, Brinker CJ. Silica nanoparticle supported lipid bilayers for gene delivery. Chem Commun (Camb). 2009; (34):5100–5102. [PubMed: 20448959]

42. Kim JJ, Sefton EC. The role of progesterone signaling in the pathogenesis of uterine leiomyoma. Mol Cell Endocrinol. 2011; 358:223–231. [PubMed: 21672608]

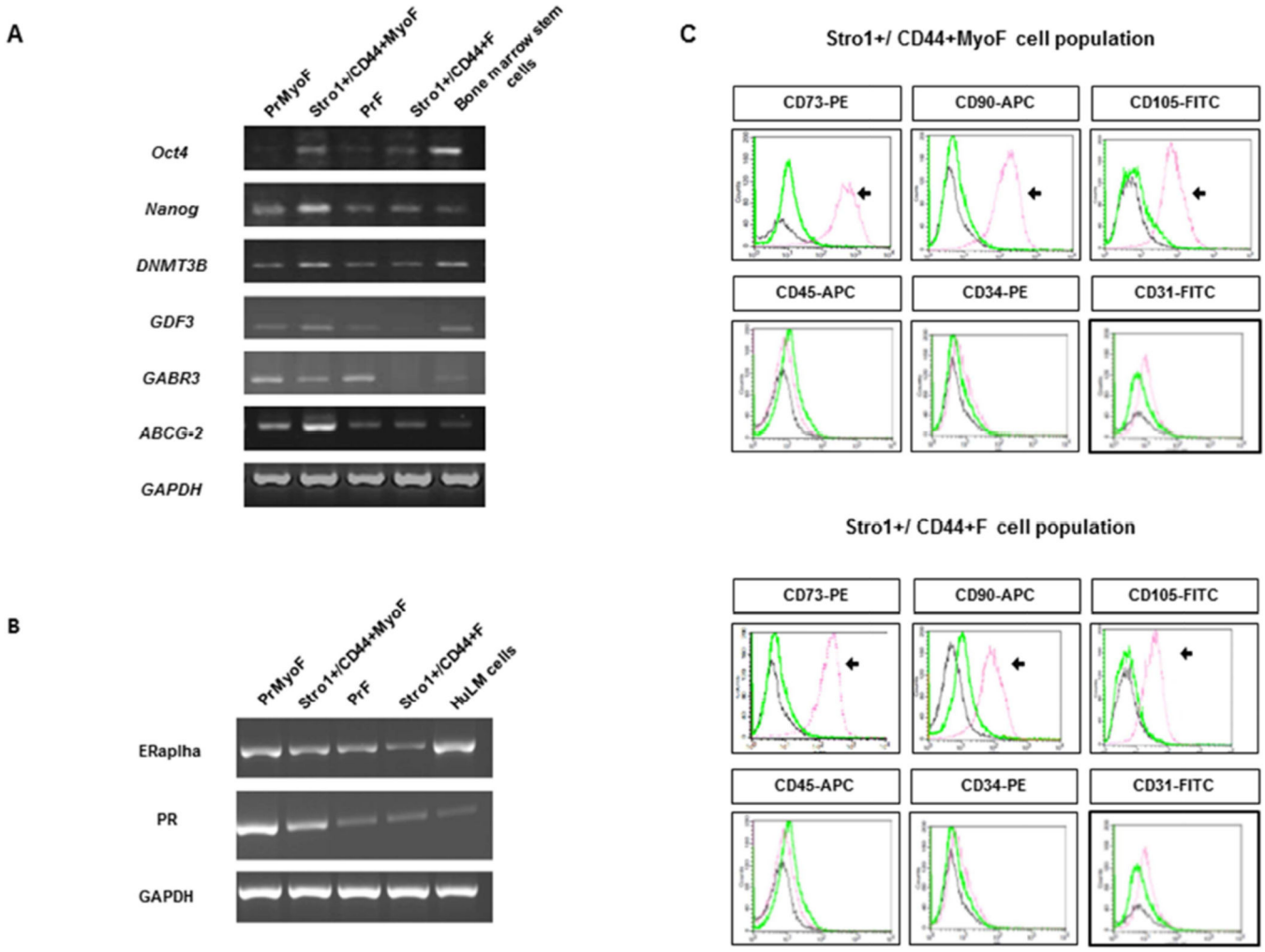

Figure 1. Molecular characterization of isolated MyoF and F stem and primary cells

(A) PCR assays demonstrating the presence and/or absence of undifferentiated genes in Stro-1^{+}/CD44^{+}MyoF/F stem cells *versus* primary cells PrMyoF/PrF **(B)** Molecular characterization showing the mRNA expression of hormonal receptors (*ERalpha*,*PR*) in primary cells PrMyoF/PrF *versus* Stro-1^{+}/CD44^{+}MyoF/F stem cells **(C)** Representative flow cytometric analysis of Stro-1^{+}/CD44^{+}MyoF/F displaying the positive expression of CD73, CD90, CD105. A negative expression of Stro-1^{+}/CD44^{+}MyoF/F was observed for hematopoietic stem cell markers (CD45 and CD34), endothelial marker (CD31).

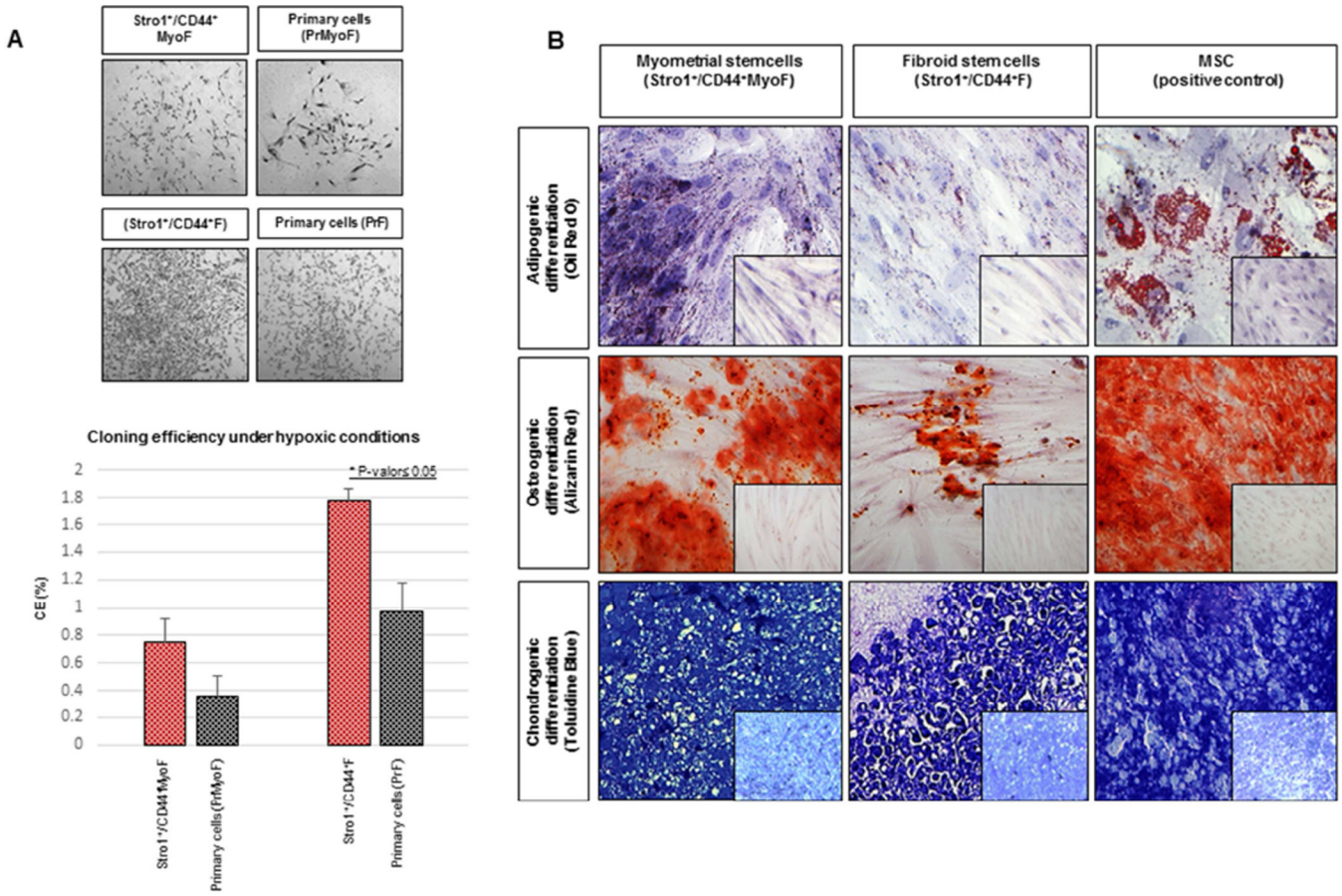

Figure 2. In vitro studies: Clonogenic assay and multipotential differentiation

(A) Highlighted macroscopic morphology showing the colonies formed by Stro-1$^+$/CD44$^+$Myo F (upper left), Stro-1$^+$/CD44$^+$F (upper right) and matching primary cells PrMyoF/PrF (lower left and right) cultured at 156 cell/cm^2 for 15 days under hypoxic conditions. Lower graph shows cloning efficiency (%) of Stro-1$^+$/CD44$^+$MyoF and Stro-1$^+$/CD44$^+$F stem *versus* primary cells PrMyoF/PrF (data are means ± SEM). **(B)** (*Upper pannel*) Induction of adipogenic differentiation detected by the presence of Oil Red-O staining in Stro-1$^+$/CD44$^+$Myo F and Stro-1$^+$/CD44$^+$F cells. (*Middle pannel*) Osteogenic differentiation of the induced Stro-1$^+$/CD44$^+$MyoF and Stro-1$^+$/CD44$^+$F cells identified by the specific Alizarin Red staining and (*Lower pannel*) induction of chondrocyte differentiation as detected by staining with Toluidine Blue. MSC cells were included as a positive control with typical Oil Red-O, Alizarin red and Toluidine Blue staining. Untreated Stro-1$^+$/CD44$^+$MyoF and Stro-1$^+$/CD44$^+$F cells were incorporated as negative controls (*see small pictures*). All histological images were examined under a 20X objective lens.

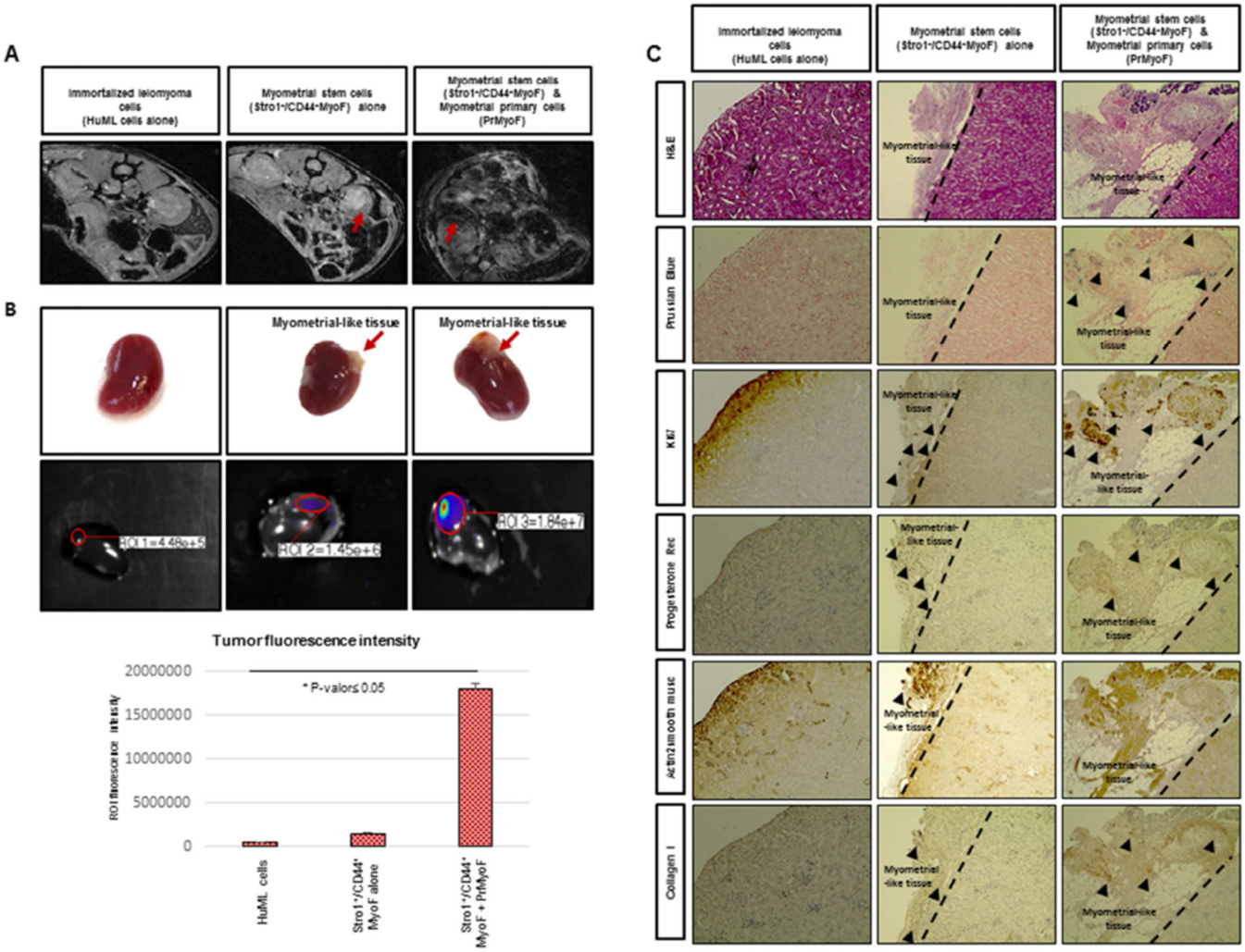

Figure 3. In vivo reconstruction of human myometrial/fibroid tissues in kidney capsule of NOD-SCID mice injected with MyoF cells

(A) In vivo xenograft imaging of mice using a magnetic resonance labeling (MRI) scanner. Scans were performed the week before to animal sacrifice and seven weeks after the injection of super-paramagnetic iron oxide (SPIO)-labeled Stro-1^{+}/CD44^{+}MyoF cells. HuML cells were used as a negative control. The recruitment of SPIO-labeled Stro-1^{+}/CD44^{+}MyoF cells resulted in decrease of signal intensity (SI) and the visualization of darker areas in xenograft sites. **(B)** Upper panels revealed the xenograft generated in the kidney capsule at macroscopic level. Middle panels represent *In vivo* xenograft imaging of mice using using the IVIS (Xenogen, Lincolnshire, United Kingdom) for 120 seconds as well the. The images obtained displayed a color spectrum, with the weakest signal being in blue and the strongest red. This intensity of signal is represented in the lower graph. **(C)** Upper panels shows the H&E staining, demonstrating the characteristic histology of fibroid-like tissue containing some adipose cells and Prussian Blue dye, allowing us to localize the human cells due to the accumulation of iron deposits. We can also appreciate the Ki67 staining, demonstrating the proliferative ability of these cells. Lower panels revealed the human Progesterone Receptor signal in the nucleus of xenograft cells from fibroid-like tissue,

suggesting the role of P4 in the growth and maintenance of leiomyoma reconstructed tissues and SMA staining, specific of smooth muscle cells. Finally, we showed the COL1A1 staining that validates the enrichment of extracellular matrix in the xenograft formed. All images were captured with a 10-fold magnification.

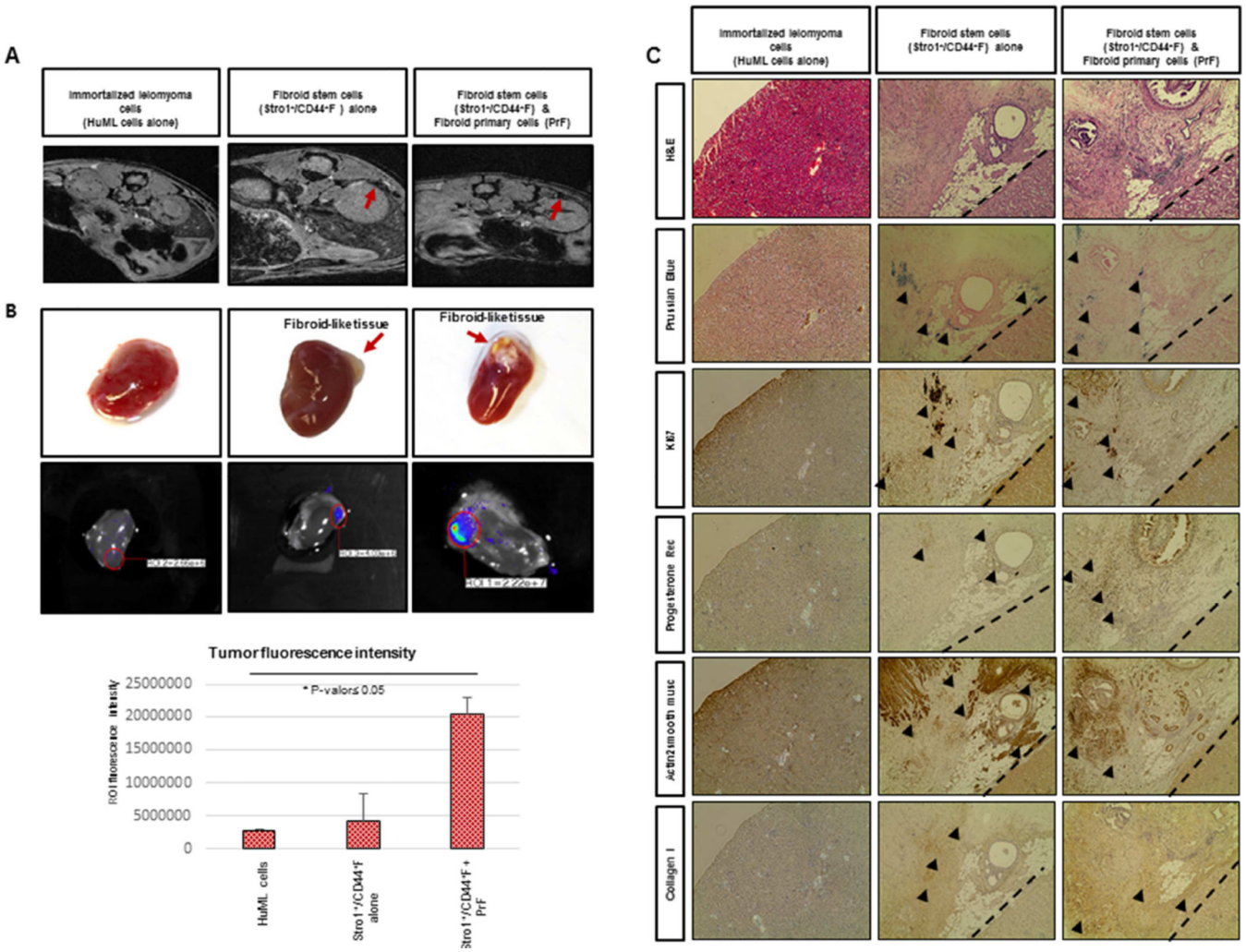

Figure 4. In vivo reconstruction of human myometrial/fibroid tissues in kidney capsule of NOD-SCID mice injected with F cells

(A) In vivo xenograft imaging of mice using a magnetic resonance labeling (MRI) scanner. Scans were performed a week prior to animal sacrifice and seven weeks after the injection of super-paramagnetic iron oxide (SPIO)-labeled Stro-1^{+}/CD44^{+}F cells. HuML cells were used as a negative control. The recruitment of SPIO-labeled Stro-1^{+}/CD44^{+}F cells resulted in decrease of signal intensity (SI) and the visualization of darker areas in xenograft sites. **(B)** Upper panels revealed the xenograft generated in the kidney capsule at macroscopic level. Middle panels represent *In vivo* xenograft imaging of mice using using the IVIS (Xenogen, Lincolnshire, United Kingdom) for 120 seconds as well the. The images obtained displayed a color spectrum, with the weakest signal being in blue and the strongest red. This intensity of signal is represented in the lower graph. **(C)** Upper panels shows the H&E staining, demonstrating the characteristic histology of fibroid-like tissue containing some adipose cells and Prussian Blue dye, allowing us to localize the human cells due to the accumulation of iron deposits. We can also appreciate the Ki67 staining, demonstrating the proliferative ability of these cells. Lower panels revealed the human Progesterone Receptor signal in the nucleus of xenograft cells from fibroid-like tissue, suggesting the role of P4 in the growth

and maintenance of leiomyoma reconstructed tissues and SMA staining, specific of smooth muscle cells. Finally, we showed the COL1A1 staining that validates the enrichment of extracellular matrix in the xenograft formed. All images were captured with a 10fold magnification.